MIMO-OFDM Acoustic Communication in Shallow Water

Lan Zhang[1,3], Taehyuk Kang[2], H.C.Song[1], W.S. Hodgkiss[1], and Xiaomei Xu[3]
[1]Scripps Institution of Oceanography, University of California, San Diego, La Jolla, California 92093-0238
[2]Qualcomm,5775 Morehouse Drive, San Diego, CA 92121
[3]School of Information and Technology, Xiamen University, Xiamen, P.R.C,361005
laz006@ucsd.edu

Abstract— **As an alternative to typical single-carrier approaches, multi-carrier Orthogonal Frequency Division Multiplexing (OFDM) communications has been explored in underwater acoustic channels with a large delay spread. In this paper, we investigate multiple-input/multiple-output (MIMO) OFDM communications that effectively can increase the data rate in band-limited underwater channels. The performance of MIMO-OFDM communications is presented using data collected from the KAM11 experiment conducted in shallow water, west of Kauai, Hawaii, which involved multiple transmit and receive arrays with a 10 kHz bandwidth (20-30 kHz) and modulations (QPSK and 16-QAM) at range up to 3 km.**

Keywords- ***MIMO-OFDM, underwater acoustic communication, single-carrier***

I. INTRODUCTION

Underwater acoustic (UWA) channels are characterized by large multipath spreads resulting in intersymbol interference (ISI) that degrades the quality of the received signal and requires channel equalization. The time varying nature of the multipath also requires continuous tracking of receiver parameters necessary for demodulation. In addition, the available bandwidth is limited due to severe frequency-dependent attenuation of the physical medium. Two common approaches to channel equalization in UWA channels are: multichannel decision-feedback equalizer (M-DFE) [2] and time reversal combining followed by a single channel DFE (TR-DFE) [3]. The two approaches are described and compared in [3] using experimental data.

Widely used in wireless channels, orthogonal frequency-division multiplexing (OFDM) recently has been introduced to UWA communication and can avoid complex channel equalization [4-7]. The basic idea is to convert a single-carrier ISI channel into parallel ISI-free sub-channels where the sub-channel (sub-carrier) bandwidth is chosen much smaller than the coherence bandwidth (i.e., inverse of the delay spread), but comparable to the channel coherence time. This is in contrast to single-carrier communication where the channel remains coherent over a large number of symbols. While OFDM enables simple equalization, well-known problems include the peak-to-average-power ratio (PAPR) and inter-carrier-interference (ICI) due to its sensitivity to Doppler effects. In addition, OFDM uses a guard period implemented as a cyclic prefix (CP) between consecutive symbols to avoid ISI. An overview of OFDM versus single-carrier transmission is provided in [8].

In an effort to increase the data throughput, multi-input and multi-output (MIMO) OFDM communication has been investigated recently at short ranges on the order of 1 km in very shallow water [9-11]. In this paper, we investigate MIMO-OFDM communications using the data collected from the KAM11 experiment conducted in shallow water (~100-m deep), west of Kauai, Hawaii, 2011 [12]. The MIMO-OFDM utilized either 2 or 4 transmitters distributed in depth while a 16-element vertical receive array was moored at 3 km range.

II. SYSTEM DESIGN

A. Transmitter design

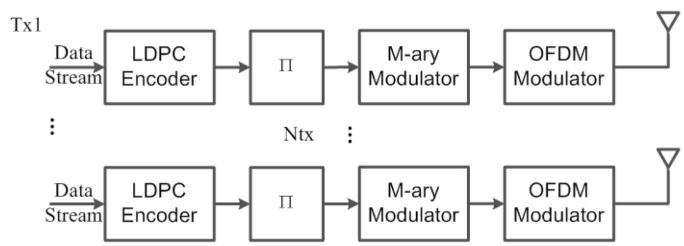

Fig . 1 Block diagram of the transmitters

As shown in Fig. 1, MIMO-OFDM communication signals were designed for either Ntx=2 or Ntx=4 transmitters using 10 kHz (10-20 kHz) bandwidth on each transmitter. The "OFDM Modulator" is made up of parallel-serial converter; IFFT; cyclic prefix (CP) adder and up-converter. The CP-OFDM format is applied with the information bits encoded by a half-rate low-density-parity-check (LDPC) code. Then the coded bits are mapped into symbols with QPSK and 16-QAM. The data stream consists of 4 packets with different carriers and different modulation: 1024-QPSK, 1024-16QAM, 2048-QPSK, and 2048-16QAM, which is shown in Fig.2. Each packet repeats four times.

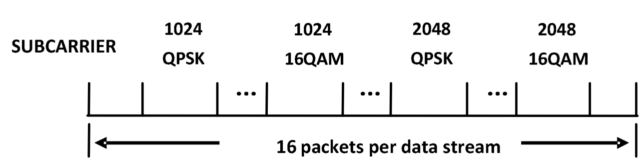

Fig . 2 The structure of data stream

978-0-933957-40-4 ©2013 MTS

Table 1 Parameters of CP-OFDM

Number of sub-carriers	N_s=2048
Number of data sub-carriers	N_d=1344
Number of pilots	N_p=512
Number of null sub-carriers	N_u=192
Cyclic duration	51.2ms
Symbol duration with CP	T_s=256ms
Subcarrier spacing	Δf= 4.88Hz
Bandwidth	10 kHz
LDPC decoder	(1344,672) Half-rate

Table 1 specifies the key parameters employed for OFDM modulation with 2048-QPSK and 2048-16QAM in the 10 kHz band (10-20 kHz). Based on the parameters, the data bits rate can be derived by

$$R_b = \log M \cdot \frac{1}{T_s} \cdot N_{tx} \cdot N_d \tag{1}$$

The packet structure is illustrated in Fig. 3. Each packet consists of 100-ms linear frequency modulated (LFM) waveform, 100-ms silence period, followed by 16 or 14 OFDM blocks with each block being 256 ms long. The total packet duration was 4.596 s for the two-transmitter case (2IMO) and 4.484 s for the four-transmitter case (4IMO). Note that the LFM waveform at the beginning of the packet is used for synchronization and Doppler shift estimation.

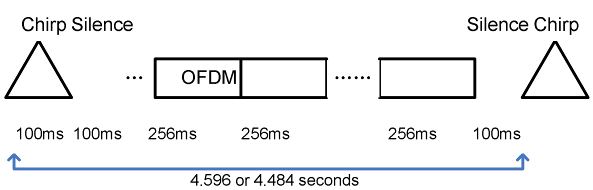

Fig . 3 Packet structure of 2048-QPSK and 2048-16QAM

B. *Receiver Design*

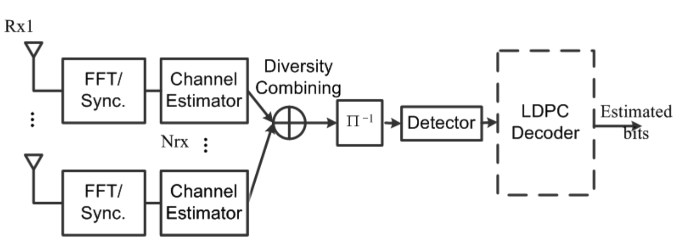

Fig . 4 Block diagram of the receiver

For stationary MIMO-OFDM data analyzed in this paper, there is no resampling required for Doppler compensation. As shown in Fig. 4, the MIMO-OFDM receiver consists of channel estimation, channel equalization, detection, diversity combining, and LDPC decoding. The number of iterations in the LDPC decoder is set to 30. Maximal Ratio Combing (MRC) is employed for diversity combining. Pilot tones are applied in order to achieve channel estimation. A linear Zero Forcing (ZF) detector and Minimum Mean Square Error (MMSE) equalization is adopted for MIMO detection. Beside the linear detection methods, we also try an ordered successive inference cancellation (OSIC) method to improve the performance [13].

We have the transmitted sequence $\boldsymbol{s}$, $\boldsymbol{s}=[s_1, s_2, \cdots s_{Ntx}]$, the received data for Nr receiver $\boldsymbol{y}$, $\boldsymbol{y}=[y_1, y_2, \cdots y_{Nr}]$, and the channel matrix $\boldsymbol{H}$ with size of $N_r \times N_{tx}$. So the received data can be obtained as:

$$\mathbf{y} = \mathbf{Hs} + \mathbf{v} \tag{2}$$

where $\mathbf{v}$ is additive noise, which is assumed to be independent on different receivers and Gaussian distributed. The equalized signals $\hat{\mathbf{s}}$ using the ZF detector based on pilot-assisted channel estimation $\hat{\mathbf{H}}$ is given by

$$\hat{\mathbf{s}} = \left(\hat{\mathbf{H}}\hat{\mathbf{H}}^{\mathbf{H}}\right)^{-1} \hat{\mathbf{H}}^{\mathbf{H}}\mathbf{y} \tag{3}$$

And the equalized data $\hat{s}$ using MMSE equalization is achieved by

$$\mathbf{W}_{\text{MMSE}} = \left[\hat{\mathbf{H}}^{\mathbf{H}}\hat{\mathbf{H}} + \mathbf{N}_0\mathbf{I}\right]^{-1} \hat{\mathbf{H}}^{\mathbf{H}} \tag{4}$$

$$\hat{\mathbf{s}} = \mathbf{W}_{\mathbf{MMSE}}\mathbf{y} \tag{5}$$

where the variance of noise is $\sigma^2 = N_0/2$ and $\boldsymbol{W}_{MMSE}$ is the MMSE weight matrix. We observe that the only difference between the two detectors is the noise spectral density factor N_0 [14].

The OSIC detector is a bank of linear receivers, each of that detects one of the parallel data streams, with the detected signal components successively canceled from the received signal at each stage. In this paper, we use MMSE method of symbol estimation and signal-interference-plus-noise-ratio (SINR)-based Ordering for OSIC detection: MMSE-SINR-OSIC method. [13] The post-detection SINR:

$$SINR_i = \frac{E(\mathbf{s})\left|\mathbf{w}_{i,MMSE}\mathbf{h}_i\right|}{E(\mathbf{s})\sum_{l \neq i}\left|\mathbf{w}_{i,MMSE}\mathbf{h}_l\right| + \sigma^2\left\|\mathbf{w}_{i,MMSE}\right\|^2}, \quad i = 1,2,\cdots N_{tx} \tag{6}$$

where $\boldsymbol{w}_{\boldsymbol{i},\boldsymbol{MMSE}}$ is the i^{th} row of the MMSE weight matrix in Equation (4), and $\boldsymbol{h}_{\boldsymbol{i}}$ is the ith column vector of the channel matrix. After ordering and MMSE filtering, the l^{th} estimated symbol with this highest SINR is found. Then the modified channel matrix after step1 is:

$$\mathbf{H}^{(step1)} = \left[\mathbf{h}_1, \mathbf{h}_2 \cdots \mathbf{h}_{l\text{-}1}, \mathbf{h}_{l+1} \cdots \mathbf{h}_{N_{tx}}\right] \tag{7}$$

With the modified channel matrix, the equations (4) and (6) are updated. It is an iterative detection. The total number of SINR calculation is $N_{tx}(N_{tx}+1)/2$.

III. EXPERIMENTAL RESULTS

A. *KAM11*

The KAM11 experiment data analyzed in this paper was collected off the western side of Kauai, Hawaii, from 23 June (JD 174) to 12 July (JD193), 2011. A schematic of the KAM11 experiment is shown in Fig. 5.

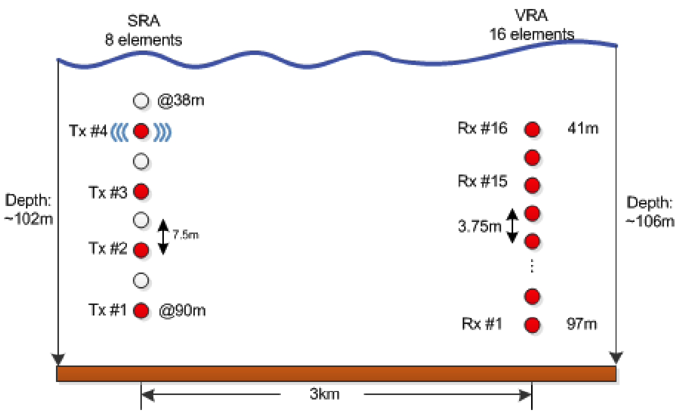

Fig . 5 Schematic of the KAM11 MIMO acoustic communication experiment

An eight-element source receiver array (SRA) was suspended in about 102m-depth water. The solid (red) dots are the transmitters used for 4IMO communication. The first transmitter was at 90 m depth. The bottom two transmitters were applied in 2IMO case. The vertical receiver array (VRA), used as the receiver, consisted of 16-elements spanning a 56m aperture with 3.75m inter-element spacing, covering about half the water column. The data were received by the VRA at a distance of 3 km. The VLA had a sampling rate of fs= 100 kHz per element.

Fig. 6 shows an example of channel responses for two transmitters in 2IMO case, which is obtained by matched filtering the probe signal (0.1 s LFM waveform from 10 kHz to 20 kHz). The channel delay spread is about 15 ms in both cases.

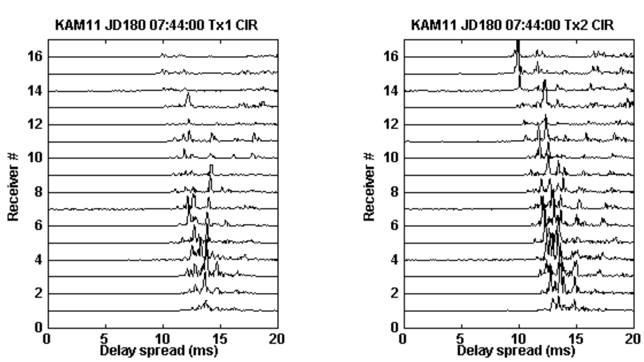

Fig . 6 An example of channel response with QPSK in 2IMO case

B. *Performance*

Table 2 summarizes the coded bit-error-rate (BER) averaged over all data bits for each transmitter in 2IMO-OFDM communications using all 16 elements of the receive array. Error-free reception can be achieved at the lower spectral efficiency (1.05b/s/Hz). For 1024-16QAM, the BER of Tx2 is shown higher than that of Tx1.

Table 2 Performance with 2 transmitters and 16 receivers

	Spectral efficiency		Average Coded BER
1024- QPSK	1.05b/s/Hz	Tx1 Tx2	0 0
1024- 16QAM	2.1b/s/Hz	Tx1 Tx2	10^{-1} $5{\cdot}10^{-2}$
2048-QPSK	1.05b/s/Hz	Tx1 Tx2	0 0
2048-16QAM	2.1b/s/Hz	Tx1 Tx2	$6{\cdot}10^{-2}$ $9{\cdot}10^{-2}$

Table 3 summarizes the coded bit-error-rate (BER) averaged over all data bits for each transmitter in 4IMO-OFDM communications. Similarly, error-free reception can be achieved at the lower spectral efficiency (2.1b/s/Hz). If the data rate increases, the BER increases to on the order of 10^{-2}.

Table 3 Performance with 4 transmitters and 16 receivers

	Spectral efficiency		Average coded BER
1024- QPSK	2.1b/s/Hz	Tx1 Tx2 Tx3 Tx4	0 0 0 0
1024- 16QAM	4.2b/s/Hz	Tx1 Tx2 Tx3 Tx4	$7{\cdot}10^{-2}$ $8{\cdot}10^{-2}$ $8{\cdot}10^{-2}$ $5{\cdot}10^{-2}$
2048-QPSK	2.1b/s/Hz	Tx1 Tx2 Tx3 Tx4	0 0 0 0

C. *Performance: Diversity combining*

In this section, the impact of diversity combing on performance is investigated. BER of 2IMO-OFDM with the 2048-QPSK packets is shown in Fig. 7 as a function of the number of receivers combined. Three different detectors are applied: ZF, MMSE and MMSE-SINR-OSIC. The 16 receivers are combined in two opposite directions: from bottom to top (solid) and then from top to bottom (dash).

As shown in Fig. 7, 4 bottom receivers can achieve error-free performance. The MMSE-SINR-OSIC curve converges faster in the direction of bottom to top. On the other hand, 11 top receivers need to be combined for error-free performance. However, the MMSE-SINR-OSIC detection is outperformed by the other two methods. The uncoded data rate is 21 kbps and the coded data rate is 10.5 kbps.

Fig. 8 displays the BER of 4IMO-OFDM with the 2048-QPSK packets as a function of the number of receivers combined. 13 bottom receivers combined achieves error-free performance. The MMSE-SINR-OSIC method still works well and converges a little faster in the direction of bottom to top. In the opposite direction, however, it is very hard for the curve to

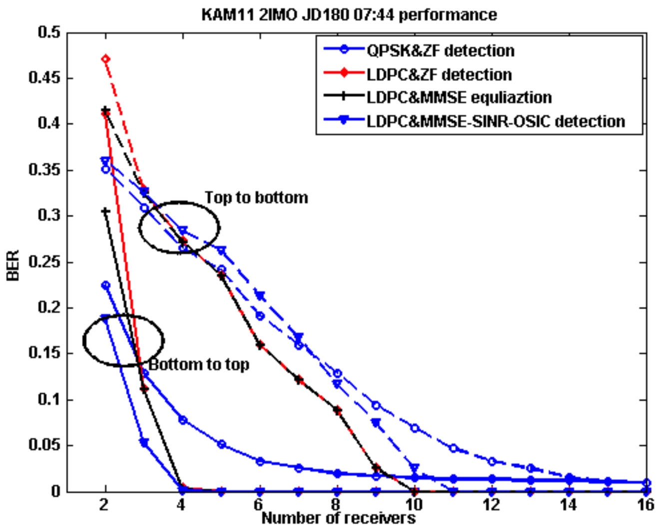

Fig . 7 BER versus the number of receive elements combined for 2IMO-OFDM transmission

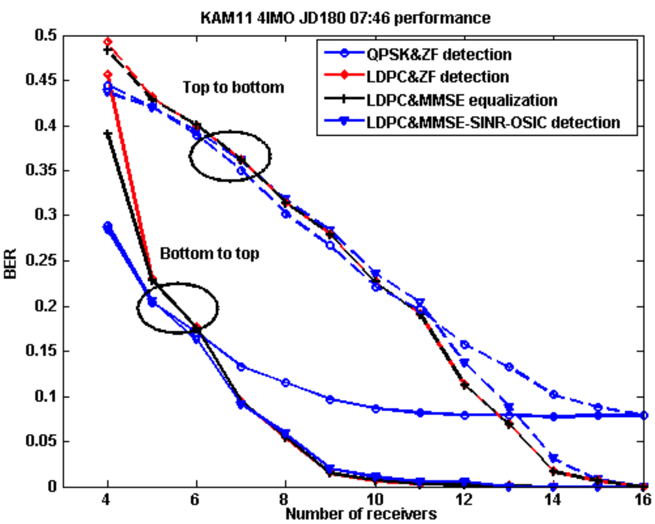

Fig . 8 BER versus the number of receive elements combined for 4IMO-OFDM transmission

SINR-OSIC detector achieves a similar performance as the other two methods. The uncoded data rate is 42 kbps and the coded data rate is 21 kbps.

As seen in the two figures above, some observations can be made. The "bottom to top" converges much faster than the "top to bottom" case because there is less refraction and reflection for propagation on the bottom and the receivers located near the bottom have higher SNR. The BER curve of QPSK does not converge due to the relatively larger errors of channel estimation. Therefore convergence must be achieved through channel coding.

IV. Conclusions

In this paper, the performance of very-high-data-rate MIMO-OFDM communication was investigated using data from KAM11 experiment conducted in shallow water. In particular, the performance of the 2IMO and 4IMO cases with two modulations (QPSK and 16-QAM) were analyzed using three different detectors: ZF detector, MMSE equalization, and MMSE-SINR-OSIC. In addition, the impact of diversity combining on performance with LDPC decoding was presented. Error-free performance was achieved using 2048-QPSK packets at a data rate of 21 kb/s.

Acknowlegement

The KAM11 experiment was supported by the Office of Naval Research. The corresponding author is grateful for the funding grants from China Scholarship Council and Research Fund for NSFC Grant No.41176032.

[1] D. Kilfoyle and A. Baggeroer, "The state of the art in underwater acoustic telemetry," IEEE J. Ocean. Eng. 25, 4-27, 2000.

[2] M. Stojanovic, A. Catipovic, and J.G. Proakis, "Reduced-complexity spatial and temporal processing of underwater acoustic communication signals", J. Acoust. Soc. Am. 98, 961-971, 1995.

[3] H.C. Song, "Time reversal communication in a time-varying sparse channel", J. Acoust. Soc. Am. 130, EL161-EL166, 2011.

[4] T. Kang and R. A. Iltis, "Iterative carrier frequency offset and channel estimation for underwater acoustic OFDM systems," IEEE J. Select.Areas Commun., 650–1661, 2008.

[5] T.Kang, H.C.Song, W.S.Hodgkiss, and J.S.Kim, "Long-range multi-carrier acoustic communications in shallow water based on iterative sparse channel estimation," J. Acoust. Soc. Am. 128, EL372-ELl377, 2010.

[6] X. Xu, Z.-H. Wang, S. Zhou, and L. Wan, "Parameterizing both path amplitude and delay variations of underwater acoustic channels for block decoding of orthogonal frequency division multiplexing," J. Acoustical Society of America., vol. 131, pp.4672-4679, Jun. 2012.

[7] X. Xu, E. Sang, N. Li, and G. Qiao, "Channel estimation algorithm in underwater acoustic communication based on DFT and OFDM," Journal of Data Acquisition & Processing, vol. 24, Jan. 2009.

[8] Z. Wang, X. Ma, and G. Giannakis, "OFDM or single-carrier block transmissions? ", IEEE Trans. Commun. 52, 380-394, 2004.

[9] Jun Tao; Zheng, Y.R.; Chengshan Xiao; Yang, T.C., "Robust MIMO Underwater Acoustic Communications Using Turbo Block Decision-Feedback Equalization," IEEE J. Oceanic Eng. 35, 948-960, 2010.

[10] B. Li, J. Huang, S. Zhou, K. Ball, M. Stojanovic, L. Freitag, and P. Willett, "MIMO-OFDM for high rate underwater acoustic communications," IEEE J. Ocean. Eng., 34, 634–644, 2009.

[11] Pelekanakis, K.; Baggeroer, A.B., "Exploiting Space–Time–Frequency Diversity With MIMO–OFDM for Underwater Acoustic Communications," Oceanic Engineering, IEEE Journal of, vol.36, no.4, pp.502, 513, Oct. 2011

[12] W.S. Hodgkiss and J. Preisig, "Kauai Acomms MURI 2011 (KAM11) experiment", in Proc. Of ECUA'12, 993-1000, 2012.

[13] YongSoo Cho, Jaekwon Kim et al., "MIMO-OFDM Wireless Communications with Matlab", John Wiley & Sons (Asia) Pte Ltd, pp:322-324,2011

[14] .J.G. Proakis ."Digital Communications", McGraw-Hill, 4thi edition, 2001